

# MORPHOMETRIC ANALYSIS OF GENETIC VARIATION IN HIPPOCAMPAL SHAPE IN MILD COGNITIVE IMPAIRMENT: ROLE OF AN IL-6 PROMOTER POLYMORPHISM

Li Shen<sup>\*1</sup>, Andrew J. Saykin<sup>2</sup>, Moo K. Chung<sup>3</sup>, Heng Huang<sup>4</sup>,  
James Ford<sup>4</sup>, Fillia Makedon<sup>4</sup>, Tara L. McHugh<sup>2</sup>, C. Harker Rhodes<sup>5</sup>

<sup>1</sup>*Computer and Info. Science, University of Massachusetts Dartmouth, N. Dartmouth, MA 02747, USA*

<sup>2</sup>*Psychiatry and Radiology, <sup>5</sup>Pathology, Dartmouth Medical School, Lebanon, NH 03756, USA*

<sup>3</sup>*Statistics, University of Wisconsin Madison, Madison, WI 53706, USA*

<sup>4</sup>*Computer Science, Dartmouth College, Hanover, NH 03755, USA*

*Email: lshen@umassd.edu, saykin@dartmouth.edu, mchung@stat.wisc.edu,*

*{hh, jford, makedon}@cs.dartmouth.edu, {tara.l.mchugh, c.harker.rhodes}@dartmouth.edu*

We study the connection between genotype and imaging phenotype in order to detect possible genetic risk factors in mild cognitive impairment (MCI) and Alzheimer’s disease (AD). We focus on identifying hippocampal shape changes related to the G allele of a common SNP of the Interleukin-6 (IL-6) gene in the -174 promoter region. In the analysis, we propose a novel surface signal extraction method and integrate it with a set of powerful surface processing techniques, including spherical harmonic surface modeling, quaternion-based 3D shape registration, and statistical inference on the surface using heat kernel smoothing and random field theory. Our analysis results in several interesting findings that suggest combining imaging phenotypes and genetic profiles has the potential to elucidate biological pathways for better understanding MCI and AD.

## 1. INTRODUCTION

Mild cognitive impairment (MCI)<sup>1</sup> is characterized by memory complaints and impairment in the absence of dementia and confers a high risk for Alzheimer’s disease (AD). Brain imaging methods for identifying medial temporal morphological abnormalities<sup>2, 3</sup> in circuits required for learning and memory have been studied for early diagnosis and treatment of MCI and AD. However, the connection between genotype and imaging phenotype has yet to be established. Doing so will facilitate identification of possible genetic risk factors for MCI and AD.

Apolipoprotein E (APOE), the one gene with a known robust association to increased risk of late-onset AD<sup>4</sup>, also appears related to subtle cognitive and neuroimaging changes well before disease onset<sup>5</sup>. Late-onset AD is a complex disorder that undoubtedly involves many genes and polymorphisms in addition to APOE. For example, the Interleukin-6 (IL-6) gene is a proinflammatory cytokine involved in neuronal signaling that appears to reduce hippocampal neurogenesis<sup>6</sup>, and the single-nucleotide polymorphism (SNP) of IL-6 in the -174 promoter region appears to modulate the reduction of medial tempo-

ral volume and gray matter concentration in older adults with memory decline<sup>7</sup>.

In this work, we extend the techniques used in combined neuromaging-genetic analysis of MCI from volumetric analysis<sup>2</sup> to shape analysis. We present a computational framework that aims to localize the interaction between morphometric changes of the hippocampus and the IL-6 -174 SNP. A novel surface signal extraction method is proposed and integrated with a set of powerful surface processing techniques<sup>8</sup>, including spherical harmonic surface modeling<sup>9</sup>, quaternion-based 3D shape registration<sup>10</sup>, and statistical inference on the surface using heat kernel smoothing and random field theory<sup>11</sup>. We hope that this surface-based shape analysis can provide important information above and beyond simple volume measurements and localize regionally specific structural changes related to the IL-6 -174 SNP in MCI.

The rest of the paper is organized as follows. Section 2 describes our method. Section 3 presents our experimental results. Section 4 concludes the paper.

## 2. METHODS

This section describes our data set as well as surface modeling, shape description, surface signal extrac-

---

\*Corresponding author.

tion, and statistical shape analysis approaches.

## 2.1. Data Set

Participants include healthy controls (HC,  $n = 40$ ), euthymic older adults with cognitive complaints (CC,  $n = 39$ ) but intact neuropsychological performance, and patients with amnesic MCI ( $n = 37$ ). Table 1 shows several participant characteristics<sup>2</sup>.

**Table 1.** Participant Characteristics

	Age (mean $\pm$ std)	Education (mean $\pm$ std)	Sex (M,F)	IL-6 (CC,CG,GG)
HC	70.6 $\pm$ 5.0	16.6 $\pm$ 2.7	12, 28	10, 13, 17
CC	72.8 $\pm$ 6.1	16.5 $\pm$ 2.7	16, 23	7, 25, 7
MCI	72.2 $\pm$ 6.9	16.4 $\pm$ 3.2	21, 16	10, 18, 9
ALL	71.8 $\pm$ 6.1	16.6 $\pm$ 2.7	49, 67	27, 56, 33

MRI scan data are acquired on a 1.5 Tesla GE scanner as a T1-weighted SPGR coronal series. The hippocampi are segmented using the BRAINS software package<sup>12</sup>. A 3D binary image of isotropic voxels is reconstructed from each set of 2D hippocampal segmentation results.

## 2.2. Surface Modeling

The spherical harmonic (SPHARM) description<sup>9</sup> is used for modeling all the hippocampal surfaces. The first step is to create a continuous and uniform mapping from the object surface to the surface of a unit sphere. It is formulated as a constrained optimization problem with the goals of topology and area preservation and distortion minimization. The result is a bijective mapping between each point  $\mathbf{v}$  on a surface and a pair of spherical coordinates  $\theta$  and  $\phi$ :  $\mathbf{v}(\theta, \phi) = (x(\theta, \phi), y(\theta, \phi), z(\theta, \phi))^T$ .

Now the object surface can be expanded into a complete set of spherical harmonic basis functions  $Y_l^m$ , where  $Y_l^m$  denotes the spherical harmonic of degree  $l$  and order  $m$ . The expansion takes the form:

$$\mathbf{v}(\theta, \phi) = \sum_{l=0}^{\infty} \sum_{m=-l}^l \mathbf{c}_l^m Y_l^m(\theta, \phi),$$

where  $\mathbf{c}_l^m = (c_{xl}^m, c_{yl}^m, c_{zl}^m)^T$ . The coefficients  $\mathbf{c}_l^m$  up to a user-desired degree can be estimated by solving a set of linear equations in a least squares fashion. The

object surface can be reconstructed using these coefficients, and using more coefficients leads to a more detailed reconstruction.

## 2.3. Shape Description

Shape information can be extracted by removing the effects of scaling, rotation and translation. To remove the scaling effect, we examine several schemes: (1) the hippocampal volume is normalized; (2) the total brain tissue volume is normalized; and (3) the intracranial volume is normalized. One of our objectives is to determine what scaling approach will be appropriate for investigating correlations between hippocampal shape and the IL6 -174 SNP and similar questions.

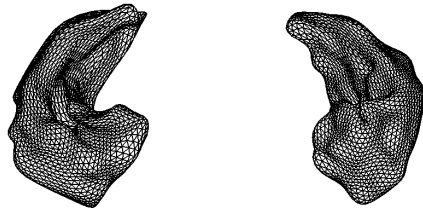


**Fig. 1.** Landmark representation for hippocampal shapes: mesh vertices are landmarks.

Rotation and translation effects can be removed by aligning 3D models to a template. Although the first order ellipsoid is often used to align SPHARM models<sup>9</sup>, it does not work for multi-object complexes. In our analysis, we want to examine not only individual shapes of left or right hippocampi but also combined left and right hippocampal complexes. To create a shape descriptor for either a single hippocampus or a two-hippocampus complex, we employ a multiple object alignment method<sup>10</sup> designed for SPHARM models. We briefly describe this method in the following paragraph.

First, the parameter space of each hippocampal surface is aligned according to the first order ellipsoid for establishing the correspondence across subjects. Next, after removing scaling (as described above), landmarks are created by a uniform sampling of one or two surfaces for each shape configuration. Finally, a quaternion-based algorithm is used to align these landmarks through least square rotation and translation: subjects are first aligned to a certain control

and then aligned to the mean shape iteratively until the mean converges. Now each hippocampus or hippocampal pair is described by a set of normalized landmarks and these landmark sets are comparable across subjects (Fig. 1).

## 2.4. Surface Signal Extraction

In order to perform statistical shape analysis, we first need to define signals or variables on the surface to describe a shape. We define the mean of all the healthy controls as our template (*i.e.*, the reference shape). Thus, the template  $\mathbf{x}_t$  can be thought of as an average and normal hippocampal shape. For an individual shape  $\mathbf{x}$ , we can directly use its deformation field  $\delta(\mathbf{x}) = \mathbf{x} - \mathbf{x}_t$  relative to the template  $\mathbf{x}_t$  to describe it. However, for each surface landmark, there are three related elements (corresponding to  $x, y, z$  coordinates) in  $\delta(\mathbf{x})$  that are needed to capture local shape changes. These elements are obviously correlated to one another, which can cause a multiple comparison issue in statistical analysis.

For simplicity, some previous studies<sup>8</sup> look at only the deformation component along the surface normal (NML) direction to reduce the number of variables considered for each landmark and remove the multiple comparison issue caused by the  $x, y, z$  coordinates. However, in most cases, this approach introduces information loss because the deformation component along the tangential plane is usually nonzero and is ignored in this case.

To minimize the information loss, we propose an alternative approach as follows. First, we perform principal component analysis<sup>13</sup> (PCA) to find the principal axis of the data (*i.e.*, the direction defined by the first principal component). After that, we use the deformation component along this direction as the surface signal. Using this approach, we can guarantee that the variance of the reduced data is maximized and the information loss is minimized.

Since our goal is to detect shape changes between two groups, we propose a second approach for surface signal extraction that examines the most “discriminative” direction. In this approach, we use Fisher’s linear discriminant<sup>13</sup> (FLD) to find such a direction; and then use the deformation component along this direction as the surface signal. FLD projects a training set consisting of two classes in our case onto

one dimension such that the ratio of between-class and within-class variability is maximized, which occurs when the FLD projection places different classes into distinct and tight clumps. Our experimental results show that the FLD direction is more sensitive than NML and PCA directions for detecting shape changes between groups.

Fig. 2 shows a sample visualization that illustrates the three surface signal extraction methods described above. The left plot includes a local submesh of our shape template. Given a data set, all the deformation fields corresponding to the submesh center are plotted as magenta stars and green circles to distinguish two shape groups. Three directions (NML in red, PCA in blue, and FLD in black) for surface signal extractions are generated based on the deformation fields. The right plot shows the deformation components along these three directions. From this plot we observe that, while PCA captures more of the data variance (*i.e.*, the mean distance from the points to the PCA line is smallest), FLD separates the deformation components better (the groups cluster better in the projection line on the right).

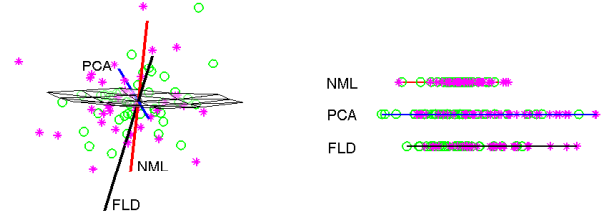


**Fig. 2.** Three methods for surface signal extraction: NML, PCA, FLD. The left plot shows a local submesh of the template, deformation fields (corresponding to the submesh center) for two shape groups (magenta stars versus green circles), and three directions (NML in red, PCA in blue, and FLD in black). The right plot shows the deformation components along the three directions.

## 2.5. Statistical Analysis

In order to increase the signal-to-noise ratio (SNR), Gaussian kernel smoothing is desirable in many statistical analyses. Since the geometry of a hippocampal surface is non-Euclidean, we cannot directly apply Gaussian kernel smoothing. Instead, we employ heat kernel smoothing, which generalizes Gaussian kernel smoothing to arbitrary Riemannian

manifolds<sup>11</sup>. Heat kernel smoothing is implemented by constructing the kernel of a heat equation on manifolds that is isotropic in the local conformal coordinates. By smoothing the data on the hippocampal surface, the SNR will increase and it will be easier to localize shape changes. Fig. 3 shows a sample heat kernel smoothing result.

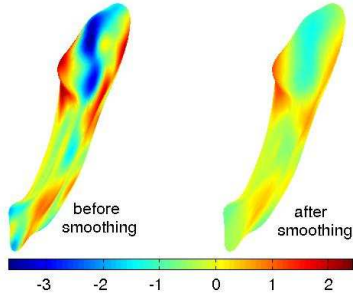


**Fig. 3.** Heat kernel smoothing: The left plot shows the initial signal mapped on to the template. The right plot shows the result after smoothing the surface using a heat kernel of FWHM = 8 mm. Our scaling scheme always makes a single hippocampus template have a volume of 3390 mm<sup>3</sup>, and the hippocampal pair template a volume of 6780 mm<sup>3</sup>.

To perform statistical inference directly on the surface, surface signals are modeled as Gaussian random fields. This theoretical model assumption has been checked using both the Lilliefors test and quantile-quantile plots for our data. Detecting the region of statistically significant shape changes can be done via thresholding the maximum of the  $t$  random field defined on the hippocampal surface. The  $p$  value of the local maxima of the  $t$  field will give a conservative threshold. See Ref. 11 for more details on how to create a corrected  $p$  value map using a  $t$  value map and other related information.

### 3. RESULTS

We perform group analyses for HC versus each possible combination of an IL-6 -174 SNP genotype (C/C, C/G, G/G) and a diagnostic group (CC, MCI). In the experiments, we use FWHM = 8mm for heat kernel smoothing. We test different scaling schemes: normalizing for hippocampal volume (HP), brain tissue volume (BV), and intracranial volume (IC). We examine not only left or right hippocampi individu-

ally but also two-hippocampus complexes. Note that the combined case is not a direct combination of two single cases. During the alignment, the spatial relation between left and right hippocampi are kept in the combined case but not in any of the single cases. We also test the NLM, PCA, and FLD surface signal extraction methods. The FLD method has the best performance; therefore, the results reported below are all based on the FLD signal extraction method.

Fig. 4 shows the resulting  $t$ -maps of several analyses using the IC scaling scheme. Positive/negative  $t$ -values indicate where inward/outward deformations of the mean shape template are required to match the second class. Note that the first class in our analyses is always HC. Statistically significant regions of shape changes only appear between HC and G/G MCI. These results suggest that the G/G MCIs are the most abnormal in shape relative to controls, while G/C and C/C genotype MCIs and CC group are unaffected in terms of hippocampal shape.

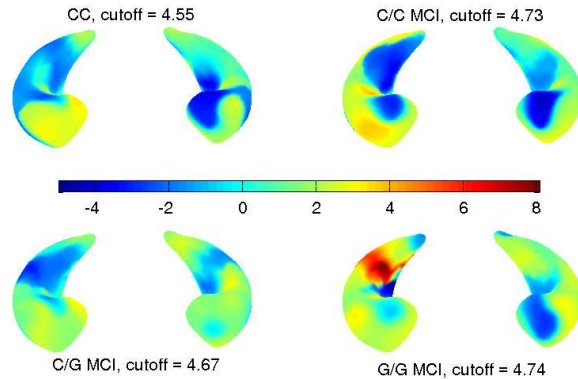


**Fig. 4.** Resulting  $t$ -maps of several analyses using IC scaling: Positive/negative  $t$ -values indicate where inward/outward deformations of the mean shape template are required to match the second class. (HC is the first class). The G/G MCIs are the most abnormal in shape relative to HCs.

In order to identify regions of statistically significant structural changes between HC and G/G MCI, we threshold the  $t$ -map at the corrected  $p$  value of 0.05 ( $t$  value of 4.74) and create a visualization shown in the top row of Fig. 5. Three different views are displayed and significant regions are shown in red and blue colors. Red/blue colors indicate where inward/outward changes to the template are needed to match G/G MCI. The shape changes of the G/G

MCI group are most pronounced in the posterior part of the right hippocampus. In this analysis, the alignment was done for hippocampal-pair complexes. The bottom row of Fig. 5 shows a very similar result using the BV scaling scheme.

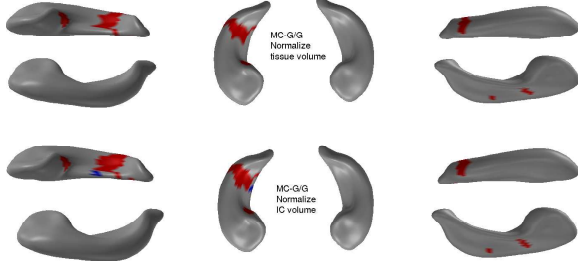


**Fig. 5.** Regions of statistically significant structural changes between HC and G/G MCI. These regions are created by thresholding the t-map using the cutoff value 4.74, which corresponds to a corrected p value of 0.05 (i.e., at 95% confidence level). Three different views are displayed. Red/blue colors indicate where inward/outward changes to the template are needed to match G/G MCI. The top and bottom rows show the results using the IC and BV scaling schemes respectively.

In another experiment, we find that shape changes are only detectable on right hippocampi for MCI participants who were homozygous for the G allele. We look at only the right hippocampi and align them separately without considering their spatial relation to the left hippocampi. We use IC scaling in this analysis. Fig. 6 shows the resulting t-maps of the analyses between HC and three MCI genotypes.

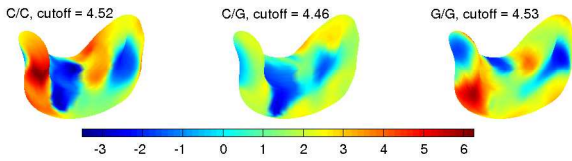


**Fig. 6.** The resulting t-maps of the analyses between HC and three MCI genotypes. Statistically significant shape changes could be identified only for MCI participants who are homozygous for the G allele, i.e., C/C MCI (left) and G/G MCI (right). All the t values in the C/G MCI analysis (middle) are well below the cutoff value 4.46

Fig. 7 shows the regions of statistically significant structural changes: (top) between HC and C/C MCI, and (bottom) between HC and G/G MCI, where the t-maps are thresholded at the corrected p value of 0.05 (t value of 4.52 for C/C MCI and 4.53

for G/G MCI). Three different views are displayed. The shape changes of both groups are located in the posterior part of the right hippocampus.

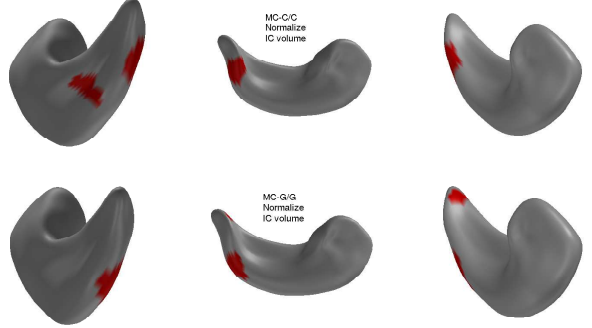


**Fig. 7.** Regions of statistically significant structural changes: (top) between HC and C/C MCI, (bottom) between HC and G/G MCI. These regions are created by thresholding the t-map using the cutoff value 4.52 for C/C MCI and 4.53 for G/G MCI, which correspond to a corrected p value of 0.05 (i.e., at 95% confidence level). Three different views are displayed. The shape changes of both groups are located in the posterior part of the right hippocampus.

Besides showing the t-maps and significant regions, we can also use the t-statistics and the surface deformation projection directions (in our case, the FLD direction) to create a shape change direction for each landmark and map it on to the template. Fig. 8 shows a sample visualization. Such a visualization can provide an intuitive, comprehensive and useful way for better understanding the connection between genotypes and imaging phenotypes.



**Fig. 8.** Visualization of shape change directions between HC and G/G MCI. The left plot shows the significant regions together with the shape change directions, while the right plot shows the directions on the whole surface. The opposite direction of each arrow suggests the deformation that is needed to match G/G MCI shape.

## 4. CONCLUSIONS

We have performed a mild cognitive impairment (MCI) study to examine hippocampal shape changes related to the IL-6 -174 SNP. In our analysis, we have proposed a novel surface signal extraction method and integrated it with a set of powerful surface processing techniques, including spherical harmonic surface modeling, quaternion-based 3D shape registration, and statistical inference on the surface using heat kernel smoothing and random field theory.

One result shows that G/G MCIs are the most abnormal in shape relative to controls, while G/C and C/C genotype MCIs and CC group are unaffected in terms of hippocampal shape. The shape changes in the G/G MCI group are most pronounced in the posterior part of the right hippocampus. Another result shows that shape changes are only identifiable on right hippocampi for MCI participants who were homozygous for the G allele; and these changes are also located in the posterior part. These findings suggest that brain imaging phenotypes, genetic profiles, and cognitive measures, in combination, have the potential to elucidate the biological pathways and circuits related to memory processes and therapeutic response in MCI and AD.

The shape changes derived from brain imaging can also be served as useful endophenotypes<sup>14</sup>, which are measurable intermediate traits that facilitate the search for genotype-phenotype associations. Thus, an interesting future topic could be to investigate a systems biology approach for understanding the genetic architecture of MCI and AD by examining more neuroimaging endophenotypes related to candidate pathways composed of ensembles of genomically distributed but functionally related genes.

## Acknowledgements

The authors thank HA Wishart, LA Rabin, LA Flashman, GJ Tsongalis, SJ Guerin, JD West, N Pare and HS Pixley of Dartmouth Medical School for their help with various aspects of this study. Supported, in part, by grants from the National Institute on Aging (R01 AG19771), Alzheimer's Association, Hitchcock Foundation, National Alliance for Medical Imaging Computing (NA-MIC, NIH U54 EB005149, NIGMS/NIH), the National Science Foundation, and UMass Healey Endowment.

## References

1. Saykin AJ, Wishart HA: Mild cognitive impairment: conceptual issues and structural and functional brain correlates. *Seminars in Clinical Neuropsychiatry*, 2003; **8**(1):12-30.
2. Saykin AJ, Wishart HA, Rabin LA, Santulli RB, Flashman LA, West JD, McHugh TL, Mamourian AC: Older adults with cognitive complaints show brain atrophy similar to that of amnesic MCI. *Neurology* 2006; in press.
3. Chen R, Herskovits EH: Network analysis of mild cognitive impairment. *NeuroImage* 2006; **29**: 1252-1259.
4. Farrer L, Cupples L, Haines J, Hyman B, Kukull W, Mayeux R: Effects of age, sex, and ethnicity on the association between apolipoprotein e genotype and Alzheimer disease: A meta-analysis, apoe and alzheimer disease meta analysis consortium. *JAMA* 1997; **278**:1349-56.
5. Wishart HA, Saykin AJ, McAllister TW, Rabin LA, McDonald BC, Flashman LA, Roth RM, Mamourian AC, Tsongalis GJ, Rhodes CH: Regional brain atrophy in cognitively intact adults with a single APOE e4 allele. *Neurology* 2006; in press.
6. Kempermann G, Kronenberg G: Depressed new neurons—adult hippocampal neurogenesis and a cellular plasticity hypothesis of major depression. *Biological Psychiatry* 2003; **54**:499-503.
7. Saykin AJ, Wishart HA, McHugh TL, Rabin LA, West JD, Yates J, Flashman LA, McAllister TW, Santulli RB, Rhodes CH: IL-6 allelic variation and medial temporal morphology in MCI and older adults with cognitive complaints. *Alzheimer's Association International Conference on the Prevention of Dementia*, 2005.
8. Shen L, Saykin A, *et. al.*: Morphometric MRI studie of hippocampal shape in MCI using spherical harmonics. *Alzheimer's Association International Conference on Prevention of Dementia*, 2005.
9. Brechbhlher C, Gerig G, Kubler O: Parametrization of closed surfaces for 3D shape description. *Comp. Vis. & Image Under.*, 1995; **61**(2):154-170.
10. Shen L, Makedon F, Saykin A: Shape-based discriminative analysis of combined bilateral hippocampi using multiple object alignment. *Medical Imaging 2004, SPIE Proc.*; **5370**:274-282.
11. Chung MK, Robbins S, Dalton KM, Davidson RJ, Alexander AL, Evans AC: Cortical thickness analysis in autism via heat kernel smoothing. *NeuroImage* 2005; **25**:1256-1265.
12. Iowa MHCRC: Brains Software Package. <http://www.psychiatry.uiowa.edu/mhrc/IPLpages/-BRAINS.htm>.
13. Duda RO, Hart PE, Stork DG. *Pattern Classification (2nd ed)*. Wiley, New York, NY, 2000.
14. Gould TD, Gottesman II: Psychiatric endophenotypes and the development of valid animal models. *Genes Brain Behav.* 2006; **5**(2):113-9.